Electronic Supplementary Material (ESI) for Polymer Chemistry.

Supplementary Information

AB_x-type amphiphilic macromonomer-based supramolecular hyperbranched polymers for controllable self-assembly

*Tingting Liu, Shuodong Wang, Yanli Song, Jiawei Li, Hongxia Yan, Wei Tian**

The Key Laboratory of Space Applied Physics and Chemistry, Ministry of Education and Shaanxi Key Laboratory of Macromolecular Science and Technology, School of Science, Northwestern Polytechnical University, Xi'an, 710072 (P. R. China)

**Correspondence to: W. Tian (e-mail: happytw_3000@nwpu.edu.cn), Tel. (fax): (+86)029-88431656*

Table of Contents

1. **Synthesis of MM**
2. **Synthesis of SHP**
3. **Self-assembly of SHP**
4. **Reversibility of SHP self-assemblies**
5. **Reference**

1 Synthesis and characterization of MM

1.1 Synthesis of oligo(GMA-EDA-*β*-CD)$_5$-≡

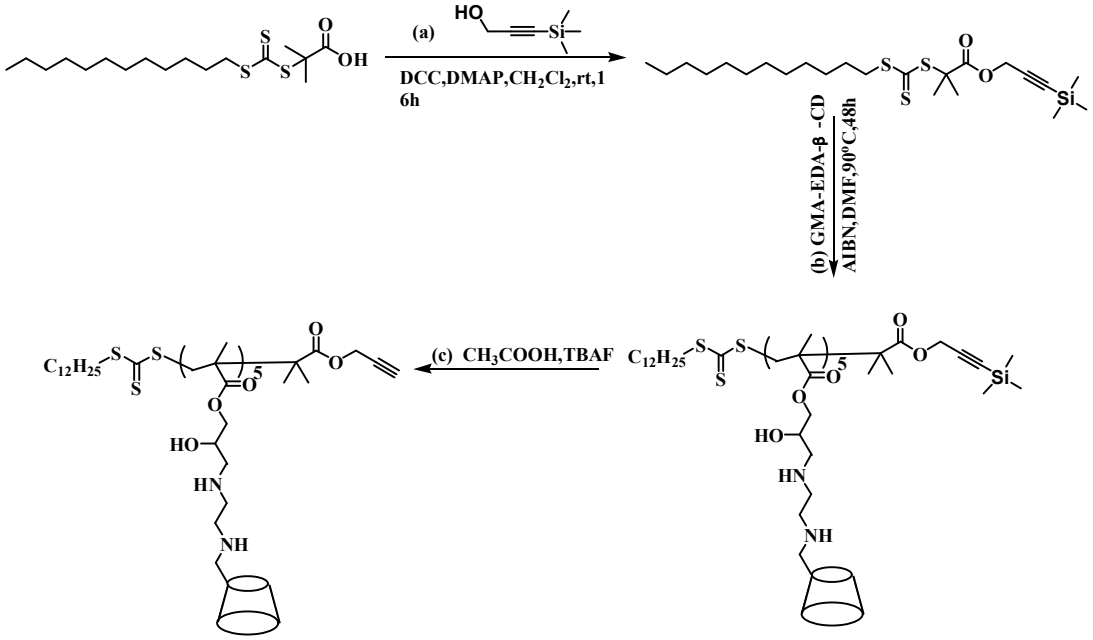

Scheme S1 Synthetic routes of dodecyl-oligo(GMA-EDA-*β*-CD)$_5$-≡.

1.1.1 Synthesis of S-1-Dodecyl-S'-(R,R'-dimethyl-R''-aceticacid) trithiocarbonate RAFT agent (DDEMETPA)

DDEMETPA was synthesized according to the literature.[S1] ^{1}H NMR ($CDCl_3$, δ, ppm): 3.31 (2H, (—CH_2—C***H$_2$***—S—); 1.99-1.56 (6H, (—COO—C(C***H$_3$***)$_2$—), (2H,—C***H$_2$***—CH_2—S—); 1.50-1.05 (18H, CH_3—(C***H$_2$***)$_9$—), 0.92 (3H, C***H$_3$***—$(CH_2)_9$—). ^{13}C NMR ($CDCl_3$, δ, ppm): 179.03 (—***C***OO—$C(CH_3)_2$—); 55.62 (—COO—***C***$(CH_3)_2$—); 31.92-25.35 (CH_3—(***C***$H_2)_{11}$—S—); 25.23 (—***C***OO—$C(CH_3)_2$—); 14.31 (***C***H_3—$(CH_2)_{11}$—S—); FTIR (KBr): 2925-2853 cm^{-1} (*m*,—CH_2—); 1730 cm^{-1} (ν, C=O); 1054 cm^{-1} (ν, C=S). Electrospray ionization mass spectrometry ($CDCl_3$, m/z): calcd for $C_{17}H_{32}O_2S_3$: 346.16; found for $[M+Na]^+$: 387.15.

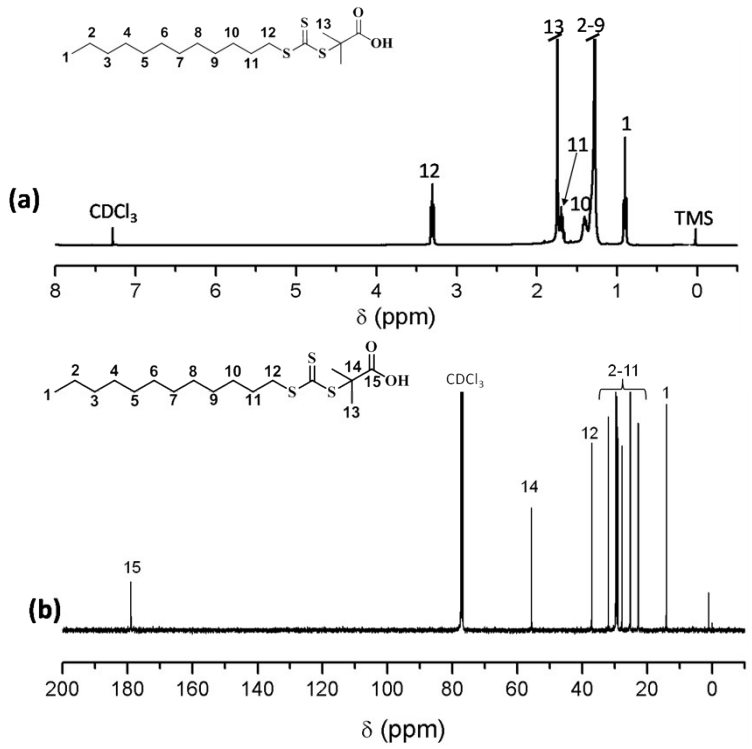

Figure S1 ^{1}H (a) and ^{13}C NMR (b) spectra of DDEMETPA

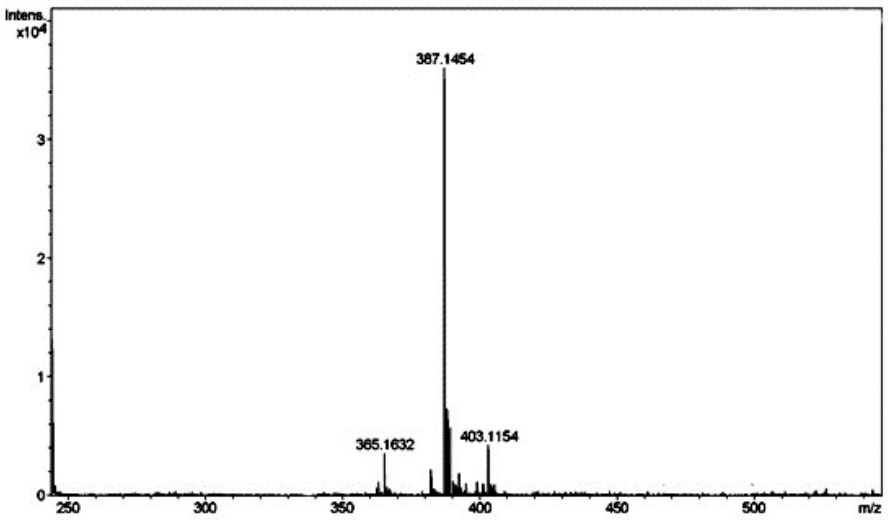

Figure S2 Electrospray ionization mass spectrum of DDEMETPA. The $(M+Na)^+$ peak was found at m/z = 387.15, which is consistent with the calculated value m/z =364.16. Additionally, the $(M+H)^+$ peak was found at m/z = 365.16, and the $(M+K)^+$ peak was found at m/z = 403.12.

1.1.2 Synthesis of 3-(Trimethylsilyl)prop-2-1-Dodecyl- 2'-(R,R'-dimethyl-R''-ethyl ester)trithiocarbonate propanoate alkyne RAFT agent (DDEMETPA-TMS)

DDEMETPA-TMS was prepared according to the literature.[4] ^{1}H NMR ($CDCl_3$, δ, ppm): 4.73 (2H, (—CH_2—C***H_2***—S—); 3.29 (2H, (—C***H_2***—CH_2—S—);1.78-

1.70 (6H, (—COO—C(C***H₃***)$_2$—); 1.47-1.21 (18H, CH_3—(C***H₂***)$_9$—), 0.9 (3H, C***H₃***—$(CH_2)_9$—); 0.21 (9H, —CH_2—C≡C—Si (C***H₃***)$_3$). ^{13}C NMR ($CDCl_3$, δ, ppm): 172.38 (—***C***OO—$C(CH_3)_2$—); 98.88 (—CH_2—***C***H≡C—$Si(CH_3)_3$); 92.33 (—CH_2—CH≡***C***—$Si(CH_3)_3$); 55.67 (—***C***H_2—CH≡C—$Si(CH_3)_3$); 54.09 (—COO—***C***$(CH_3)_2$—); 29.63-28.87 (CH_3—(***C***$H_2)_{11}$—S—); 14.15 (***C***H_3—$(CH_2)_{11}$—S—); 1.02 (—CH_2—CH≡C—Si(***C***$H_3)_3$). FTIR (KBr): 2925-2853 cm^{-1} (*m*,—CH_2—); 2186 cm^{-1} (ν, C≡C); 1742 cm^{-1} (ν, C=O); 1250 cm^{-1} (ν,—Si—); 1054 cm^{-1} (ν, C=S). Electrospray ionization mass spectrometry ($CDCl_3$, m/z): calcd for $C_{22}H_{40}O_2S_3Si$: 474.2; found for $[M+Na]^+$: 497.2.

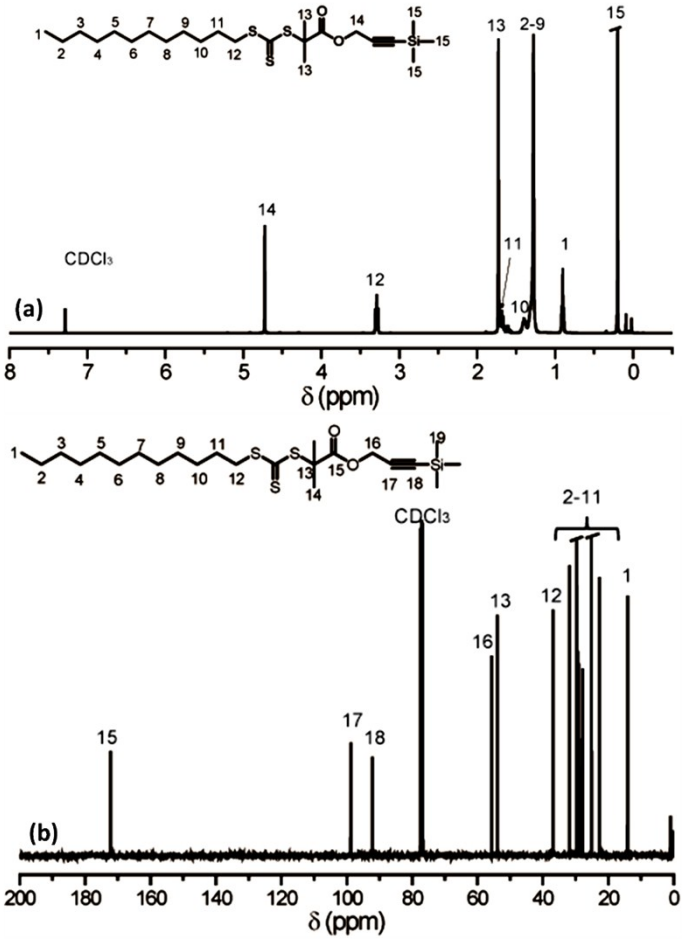

Figure S3 ^{1}H (a) and ^{13}C NMR (b) spectra of DDEMETPA-TMS.

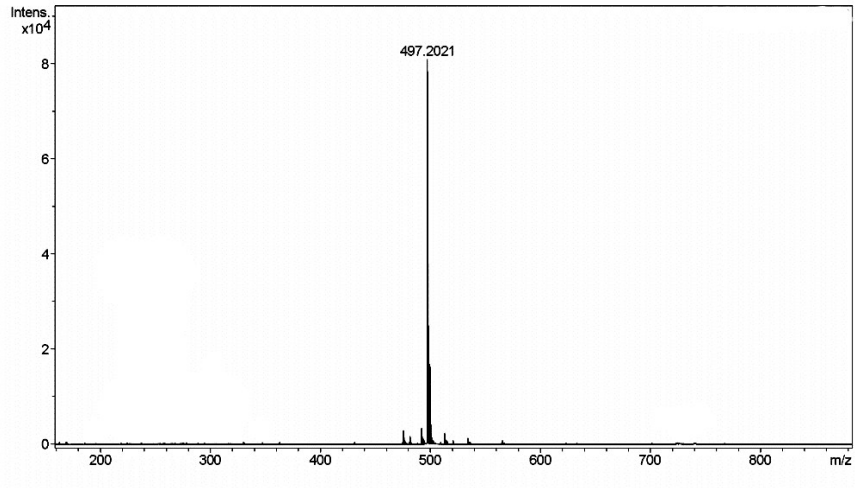

Figure S4 Electrospray ionization mass spectrum of DDEMETPA-TMS. The $(M+Na)^+$ peak was found at m/z = 497.2 which is consistent with the calculated value m/z =474.2.

1.1.3 Synthesis of dodecyl-oligo(GMA-EDA-*β*-CD)$_5$-TMS

Dodecyl-oligo(GMA-EDA-*β*-CD)$_5$-TMS was synthesized by RAFT. DDEMETPA-TMS (47.4mg, 0.1 mmol), GMA-EDA-*β*-CD (1318 mg, 1 mmol), AIBN (1.64 mg, 0.01 mmol) was dissolved in dried DMF (2 ml). The mixture was then stirred for 5 min and subjected to three freeze-vacuum-thaw cycles, and then the tube was immersed into an oil bath at 90 ^oC to perform polymerization. The mixture was dialyzed (molecular weight cut off: 3500) for 5 d. Dodecyl-oligo(GMA-EDA-*β*-CD)$_5$-TMS was obtained by lyophilization. Yields: 43%. ^1H NMR (DMSO-d_6, δ, ppm): 6.11-5.55 (50H, 2,3-OH); 5.05-4.70 (35H, 1-H); 4.60-4.35 (35H, 6-OH); 3.80-3.10 (175H, 3,5,6-H and 2,4-H); 1.25 (6H, —C(C***H*****$_3$**)$_2$—COO—); 0.21 (9H, —CH_2—C≡C—Si (C***H*****$_3$**)$_3$). ^{13}C NMR (DMSO-d_6, δ, ppm): 162.07 (—C(CH_3)—***C***OO—CH_2— and —C(CH_3)$_2$—***C***OO—CH_2—); 101.94 (C-1); 81.46 (C-4); 72.48 (C-2,3,5); 60.03 (C-6); 35.54 (—C(CH_3)—COO—***C***H_2—); 30.77-14.03 (—C(***C***H_3)—COO—CH_2—, CH_3—(***C***H_2)$_{11}$—S—); 1.02 (—CH_2—C≡C—Si(***C***H_3)$_3$)). FTIR (KBr): 3300 cm^{-1} (ν,—

OH); 1640 cm^{-1} (ν, C=O); 810 cm^{-1} (ν, C—Si). $M_{n,SEC/MALLS}$=10400, $M_{w,SEC/MALLS}$=13200, M_w/M_n=1.27.

1.1.4 Synthesis of dodecyl-oligo(GMA-EDA-β-CD)$_5$-≡

Silyl deprotection was carried using a modified procedure reported by Haddleton et al.[5] Protected dodecyl-oligo(GMA-EDA-β-CD)$_5$-TMS (300 mg) was dissolved in DMF (10 mL) and the vial purged with nitrogen for 10 minutes. Acetic acid (10 mol%) was added and the solution was cooled to -20 ^oC. TBAF in THF (10 eq.) was added dropwise to the polymer solution and the reaction mixture was stirred at -20 ^oC for 30 minutes followed by stirring at room temperature for 16 hours. The mixture was dialyzed (molecular weight cut off: 3500) for 5 d. Dodecyl-oligo(GMA-EDA-β-CD)$_5$-≡ was obtained by lyophilization. Yields: 43%. ^{1}H NMR (DMSO-d_6, δ, ppm): 6.11-5.55 (50H, 2,3-OH); 5.05-4.70 (35H, 1-H); 4.60-4.35 (35H, 6-OH); 3.80-3.10 (175H, 3,5,6-H and 2,4-H); 2.30 (1H, —CH_2—C≡C***H***) ; 1.25 (6H, —C(C***H***$_3$)$_2$—COO—). ^{13}C NMR (DMSO-d_6, δ, ppm): 162.07 (—C(CH_3)—***C***OO—CH_2— and —C(CH_3)$_2$—***C***OO—CH_2—); 101.94 (C-1); 81.46 (C-4); 72.48 (C-2,3,5); 60.03 (C-6); 35.54 (—C(CH_3)—COO—***C***H_2—); 30.77-14.03 (—C(***C***H_3)—COO—CH_2—, CH_3—(***C***H_2)$_{11}$—S—). FTIR (KBr): 3300 cm^{-1} (ν,—OH); 1640 cm^{-1} (ν, C=O). $M_{n,SEC/MALLS}$=10200, $M_{w,SEC/MALLS}$=13100, M_w/M_n=1.29.

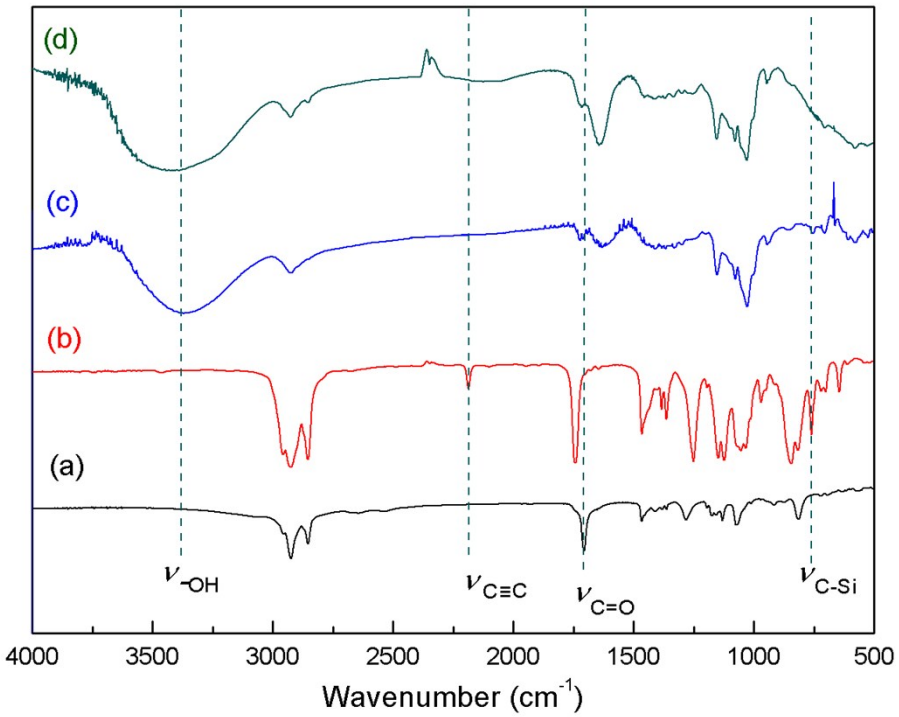

Figure S5 FTIR spectra of DDMAT (a), DDEMETPA-TMS (b), dodecyl-oligo(GMA-EDA-*β*-CD)$_5$-TMS (c), and dodecyl-oligo(GMA-EDA-*β*-CD)$_5$-≡ (d).

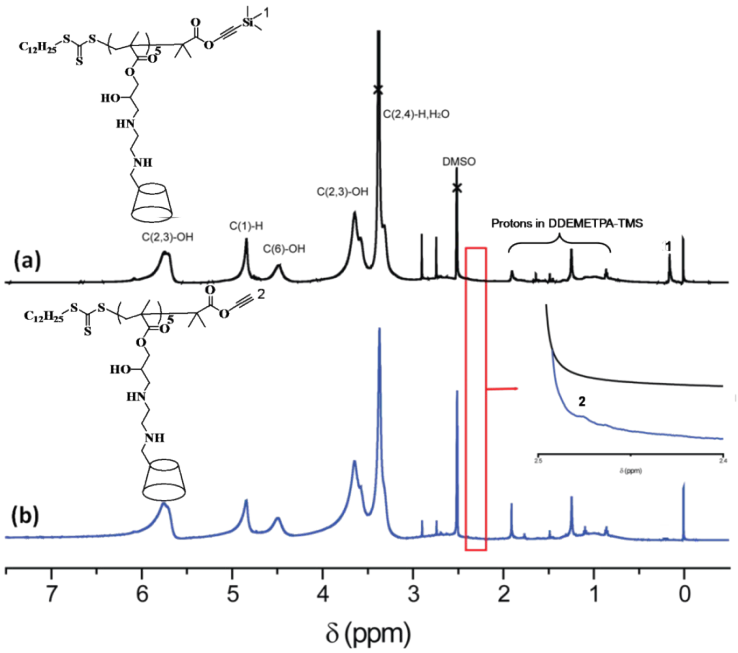

Figure S6 ^{1}H NMR spectra of dodecyl-oligo(GMA-EDA-*β*-CD)$_5$-TMS (a) and dodecyl-oligo(GMA-EDA-*β*-CD)$_5$-≡ (b)

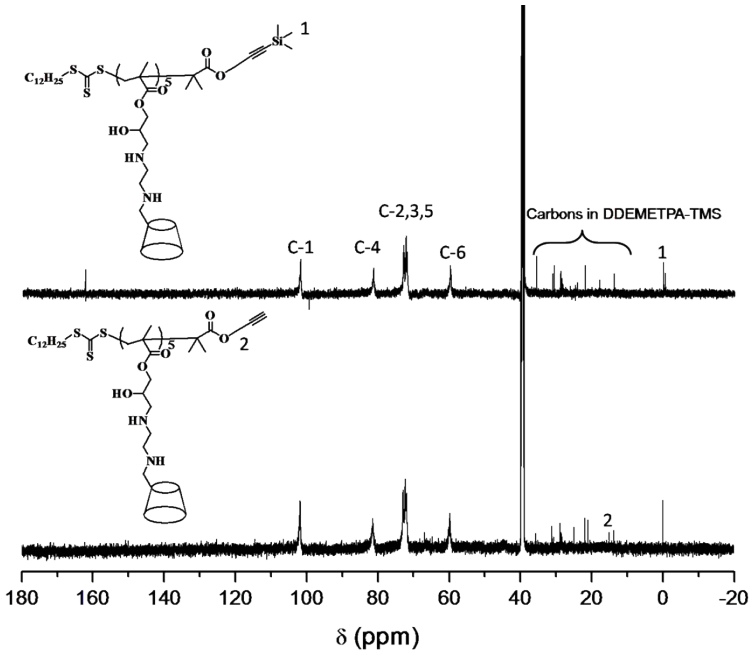

Figure S7 ^{13}C NMR spectra of dodecyl-oligo(GMA-EDA-*β*-CD)$_5$-TMS (a) and dodecyl-oligo(GMA-EDA-*β*-CD)$_5$-≡ (b)

1.2 Synthesis of *t*Azo-PDMA-N_3

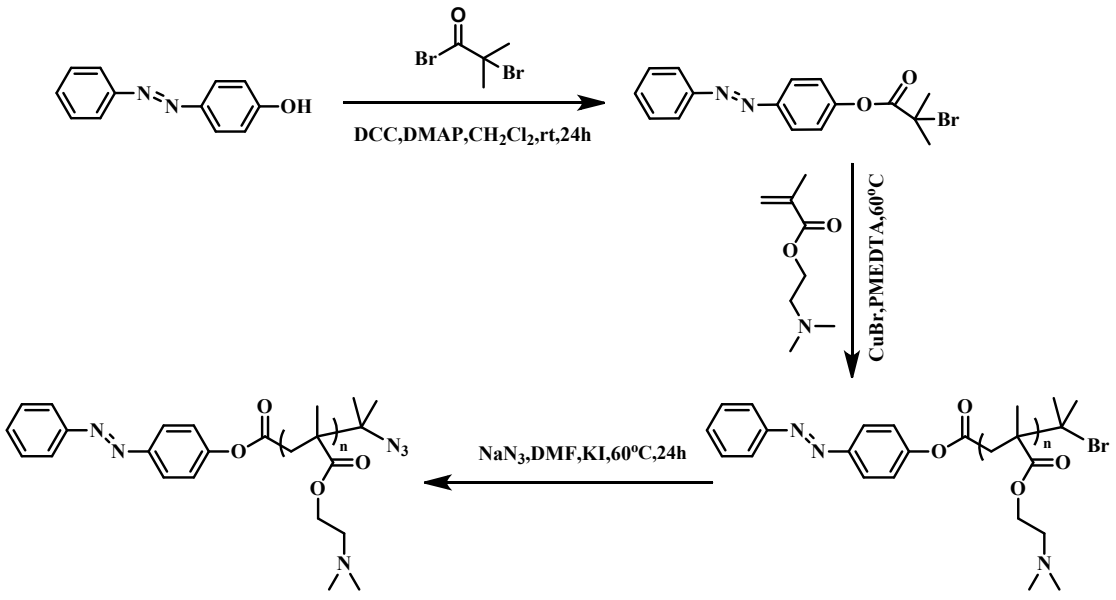

Scheme S2 Synthetic routes of *t*Azo-PDMA$_{23}$-N_3

1.2.1 Sythesis of 2-Bromo-2-methylpropionyl ester Azobenzene (BMPE-Azo)

BMPE-Azo was synthesized by the esterification reaction of 4-phenylAzophenol and 2-Bromo-2-methylpropionyl bromide. 4-phenylAzophenol (1.03 g, 5.2 mmol), 4-dimethylaminopyridine (157 mg, 1.3 mmol), pyridine (449 mg, 5.7 mmol) was dissolved in dried CH_2Cl_2 (20 ml). After cooling to 0 ^oC, 2-bromo-2-methylpropionyl bromide (715 mg, 5.7 mmol) was added dropwise to the solution. The mixture was then stirred at room temperature for 24 h. After completion of strring, deionized water (100 mL) was added in the mixture. The organic solution was washed with deionized water three times. After the organic solution was dried with anhydrous sodium sulfate, the CH_2Cl_2 was removed by rotary evaporator. The crude product was purified by column chromatography (silica gel size: 70-100 μm, column diameter: 7 cm, column length: 30 cm) using petroleum acetone/diethyl ether (V/V=9/1) as elute, yielding orange solid. Yields: 75%. ^1H NMR ($CDCl_3$, δ, ppm): 7.98-7.54 (9H, proton in azobenzene); 2.11 (6H, —C(C***H*****3**)**2**—Br). ^{13}C NMR ($CDCl_3$, δ, ppm): 170.19 (—***C***OO—$C(CH_3)_2$—Br); 152.75-119.97 (carbons in azobenzene); 62.96 (—COO—***C***H$(CH_3)_2$); 32.55 (—COO—C(***C***$H_3)_2$—Br). FTIR (KBr): 1640 cm^{-1} (ν, C=O); 519 cm^{-1} (ν, C—Br). Electrospray ionization mass spectrometry ($CDCl_3$, m/z): calcd for $C_{16}H_{15}O_2N_2Br$: 346.02; found for $[M+Na]^+$: 369.02.

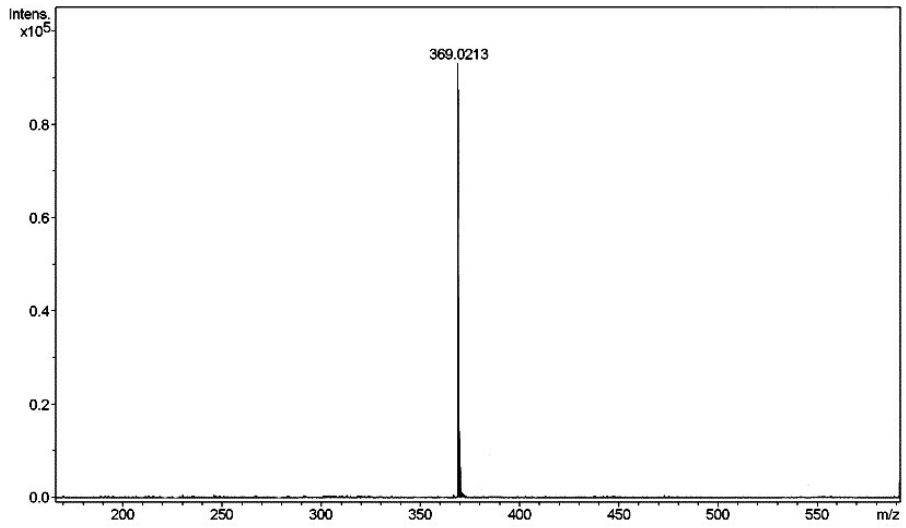

Figure S8 Electrospray ionization mass spectrum of BMPE-Azo. The $(M+Na)^+$ peak was found at m/z = 369.02 which is consistent with the calculated value m/z =346.02. Additionally, the $(M+H)^+$ peak was found at m/z = 347.04.

1.2.2 Synthesis of *t*Azo-PDMA$_{23}$-Br

A Schlenk tube was added with DMA (1260 mg, 8 mmol), PMEDTA (70 mg, 0.4 mmol), CuBr (58 mg, 0.4 mmol), BMPE-Azo (121 mg, 0.4 mmol) and dry DMF (1 ml) under nitrogen. The mixture was then stirred for 5 min and subjected to three freeze-vacuum-thaw cycles, and then the tube was immersed into an oil bath at 60 °C to perform polymerization. After 2 h, the mixture was diluted with THF and passed though a neutral alumina column. The collected eluents were concentrated and precipitated into an excess of n-hexane. Yields: 65.1%. ^{1}H NMR ($CDCl_3$, δ, ppm): 7.92-7.54 (9H, protons in azobenzene); 4.09 (46H, —COO—CH_2—C***H*****$_2$**—N—); 2.59 (46H, —COO—C***H*****$_2$**—CH_2—N—); 2.30 (138H, —CH_2—CH_2—N(C***H*****$_3$**$)_2$); 2.03-1.77 (46H, —CH(CH_3)—C***H*****$_2$**—); 1.27 (6H, —C(C***H*****$_3$**$)_2$—Br); 1.16-0.75 (69H, —CH(C***H*****$_3$**)—CH_2—). ^{13}C NMR ($CDCl_3$, δ, ppm): 170.19 (—***C***OO—CH_2—CH_2—, —***C***OO—C($CH_3$$)_2$—); 129.01-120.48 (carbons in azobenzene); 62.97 (—COO—

CH(CH_3)$_2$); 57.16 (—COO—***C***H$_2$—CH$_2$—N—, —COO—CH$_2$—***C***H$_2$—N—); 46.02 (—CH$_2$—CH$_2$—N(***C***H$_3$)$_2$); 45.01 (—CH(***C***H$_3$)—CH$_2$—); 32.55 (—COO—C(***C***H$_3$)$_2$—Br). FTIR (KBr): 1710 cm^{-1} (ν, —COO—); 519 cm^{-1} (ν, C—Br). $M_{n,SEC/MALLS}$=8800, $M_{w,SEC/MALLS}$=9100, M_w/M_n=1.04.

1.2.3 Synthesis of *t*Azo-PDMA$_{23}$-N$_3$

*t*Azo-PDMA$_{23}$-N$_3$ was obtained by the azidation of *t*Azo-PDMA$_{23}$-Br. The typical procedure was as follows. *t*Azo-PDMA$_{23}$-Br (240 mg, 0.02 mmol), NaN$_3$ (26 mg, 0.4mmol) was mixed with DMF (2 ml). The mixture was stirred at 50 ^{o}C for 48 h. After cooling to room temperature, the mixture was diluted with THF and passed though a neutral alumina column. The collected eluents were concentrated and precipitated into an excess of n-hexane. Yields: 80.1%. ^{1}H NMR (CDCl$_3$, δ, ppm): 7.92-7.54 (9H, proton in azobenzene); 4.05 (46H, —COO—CH$_2$—C***H$_2$***—N—); 2.56 (46H, —COO—C***H$_2$***—CH$_2$—N—); 2.28 (138H, —CH$_2$—CH$_2$—N(C***H$_3$***)$_2$); 2.10-1.68 (46H, —CH(CH$_3$)—C***H$_2$***—); 1.25 (6H, —C(C***H$_3$***)$_2$—Br); 1.24-0.64 (69H, —CH(C***H$_3$***)—CH$_2$—). ^{13}C NMR (CDCl$_3$, δ, ppm): 170.19 (—***C***OO—CH$_2$—CH$_2$—, —***C***OO—C(CH$_3$)$_2$—); 129.01-120.48 (carbons in azobenzene); 62.97 (—COO—***C***H(CH$_3$)$_2$); 57.16 (—COO—***C***H$_2$—CH$_2$—N—, —COO—CH$_2$—***C***H$_2$—N—); 46.02 (—CH$_2$—CH$_2$—N(***C***H$_3$)$_2$); 45.01 (—CH(***C***H$_3$)—CH$_2$—); 32.55 (—COO—C(***C***H$_3$)$_2$—Br). FTIR (KBr): 2204 cm^{-1} (ν, N$_3$); 1710 cm^{-1} (ν, —COO—).

$M_{n,SEC/MALLS}$=8500, $M_{w,SEC/MALLS}$=9500, M_w/M_n=1.12.

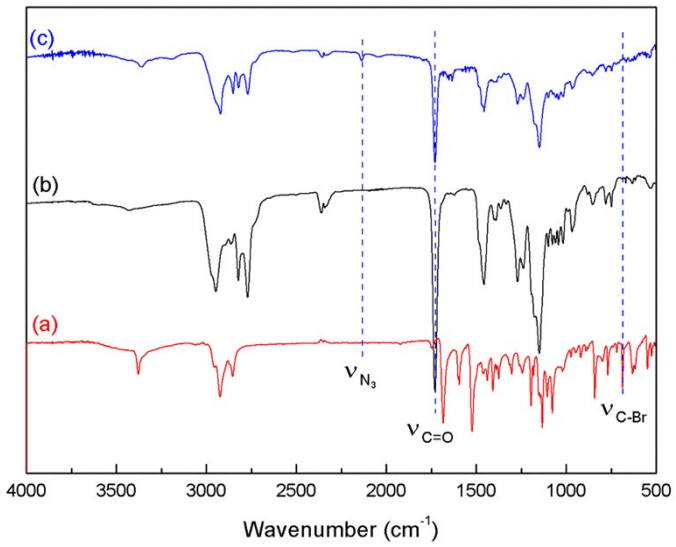

Figure S9 FTIR spectra of BMPE-Azo (a), *t*Azo-PDMA$_{23}$-Br (b), and *t*Azo-PDMA$_{23}$-N$_3$ (c)

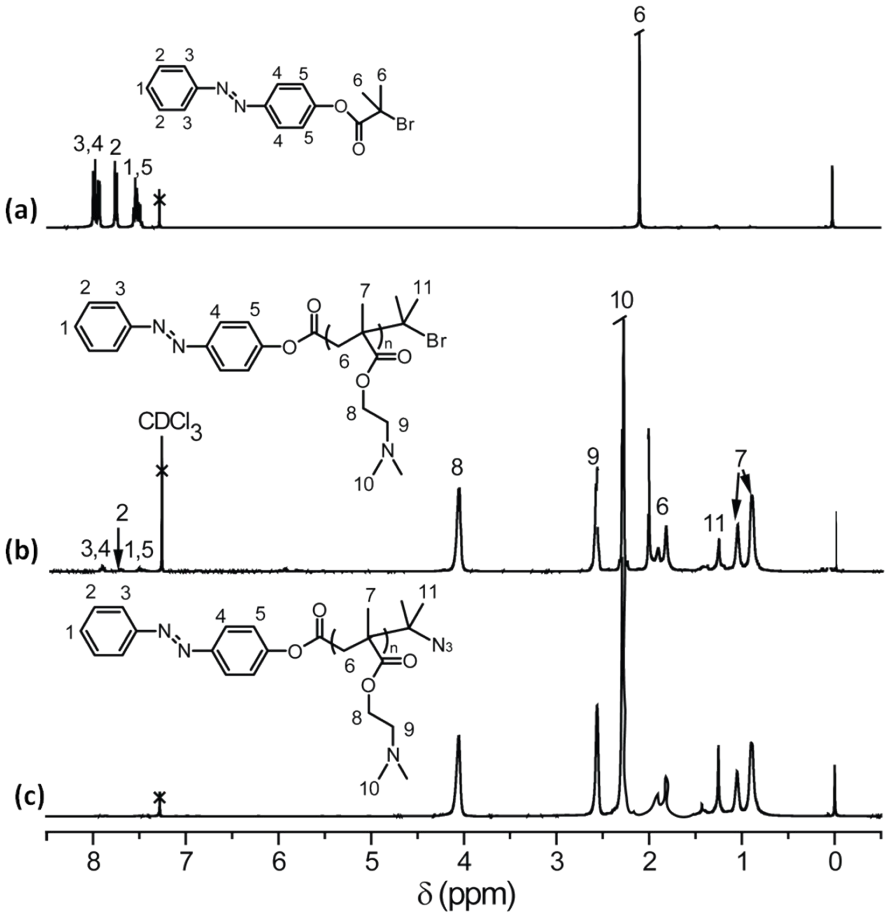

Figure S10 ^{1}H NMR spectra of BMPE-Azo (a), *t*Azo-PDMA$_{23}$-Br (b), and *t*Azo-PDMA$_{23}$-N$_3$ (c)

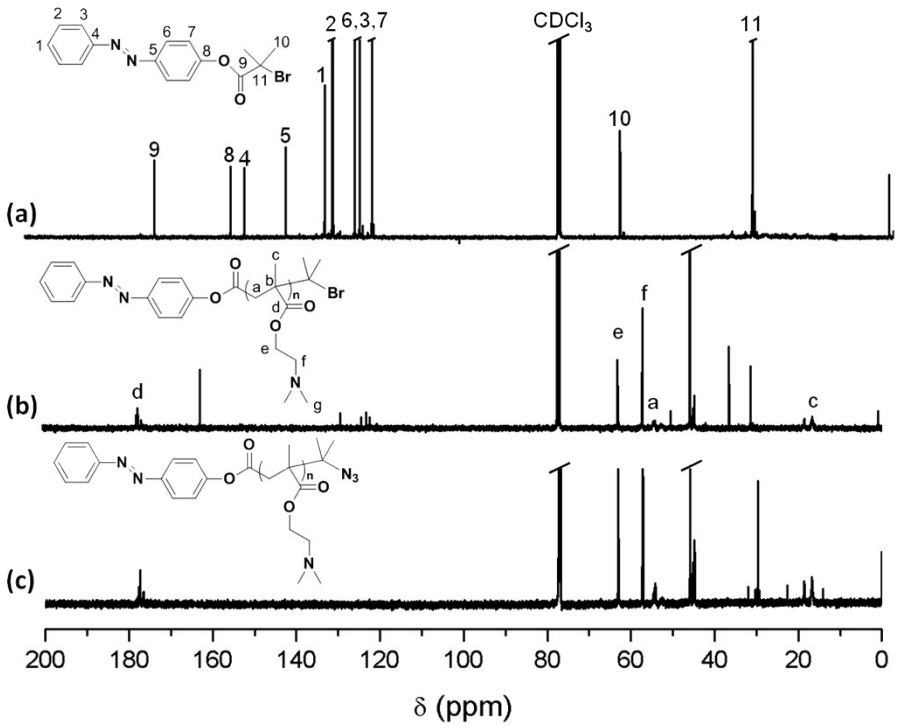

Figure S11 ^{13}C NMR spectra of BMPE-Azo (a), *t*Azo-PDMA$_{23}$-Br (b), and *t*Azo-PDMA$_{23}$-N$_3$ (c)

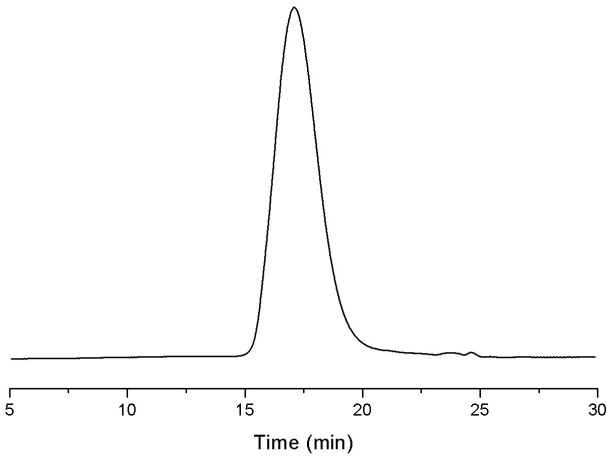

Figure S12 SEC-MALLS curve of *t*Azo-PDMA$_{23}$-Br

1.3 Synthesis of MM

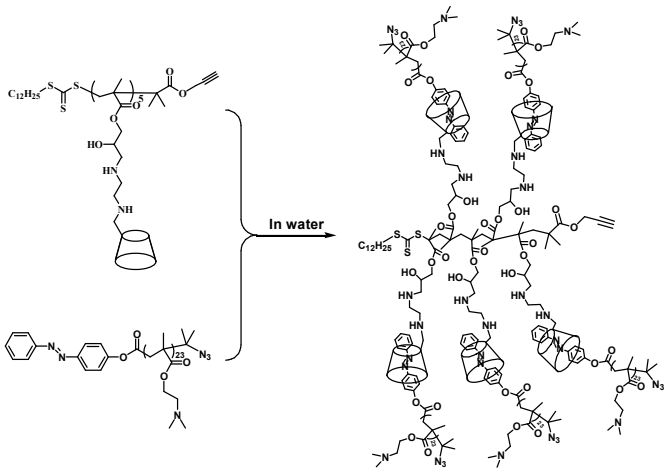

Scheme S3. Synthetic route of AB_x-type macromonomer.

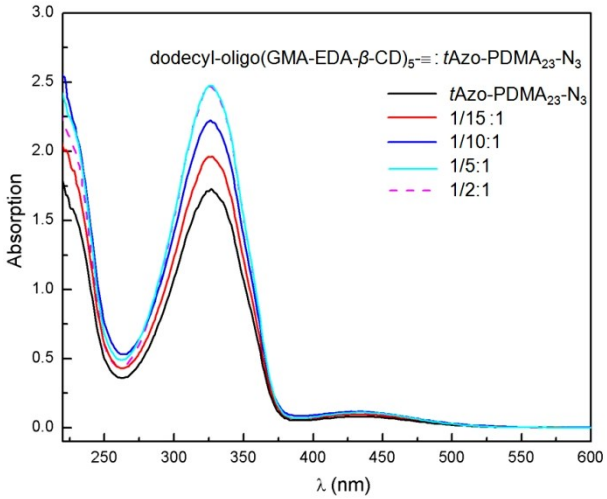

Figure S13 UV absorption of *t*Azo-$PDMA_{23}$-N_3 upon stepwise addition of dodecyl-oligo(GMA-EDA-*β*-CD)$_5$-≡ (The concentration of dodecyl-oligo(GMA-EDA-*β*-CD)$_5$-≡ is 2.55×10^{-4} M).

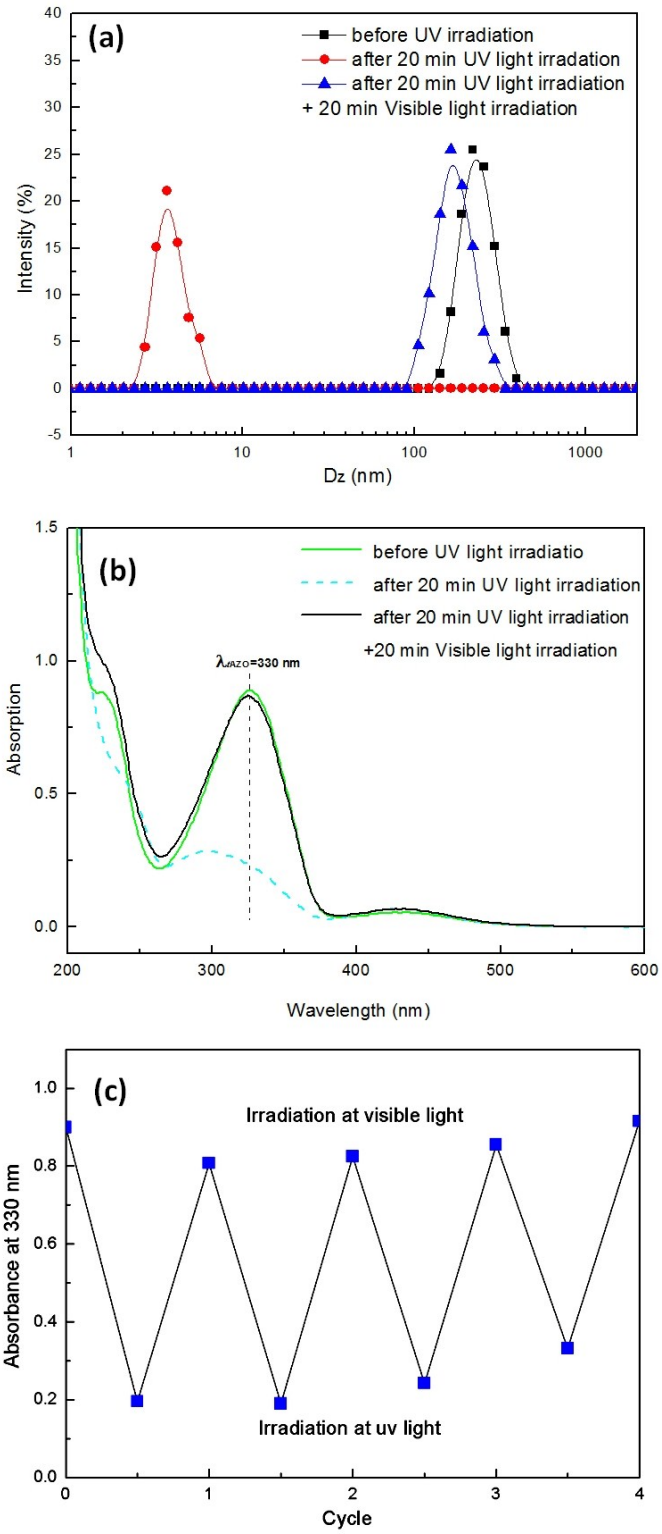

Figure S14 (a) Hydrodynamic diameter distribution of MM solutions (1.0 mg·ml^{-1}): initial state (black line); after 365 nm UV irradiation for 20 min (red line) and after 450 nm visible light irradiation for 20 min (blue line). (b) UV-vis spectra of MM solutions: before (green line) and after (blue line) UV light irradiation, after UV and visible light irradiation (black line). (c) Cycle change of absorption values at 330 nm of MM solutions by alternately imposing UV and visible light irradiation.

2 Synthesis of SHP

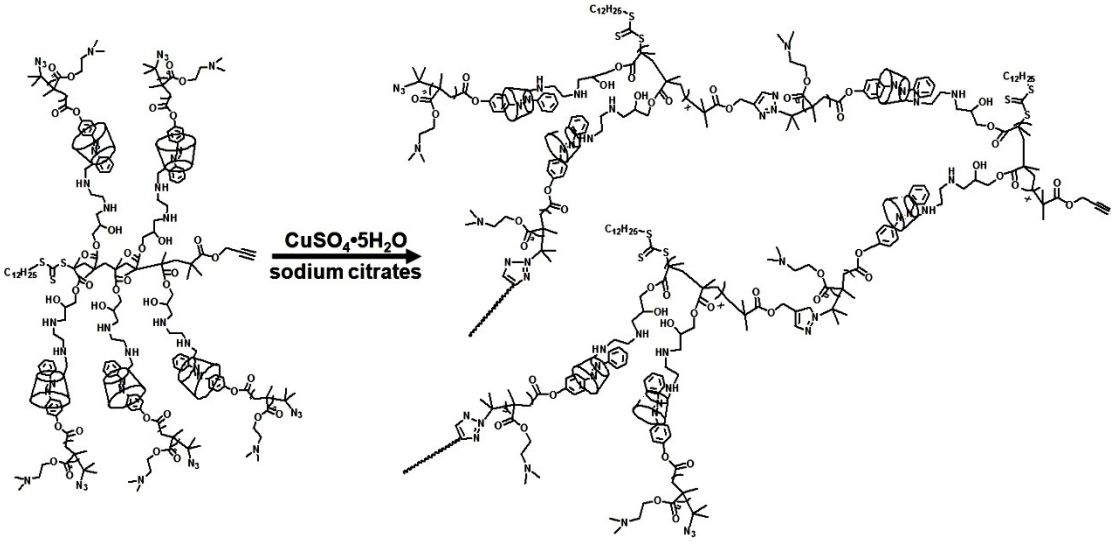

Scheme S4 Synthetic route of SHP.

3. Self-assembly of SHP

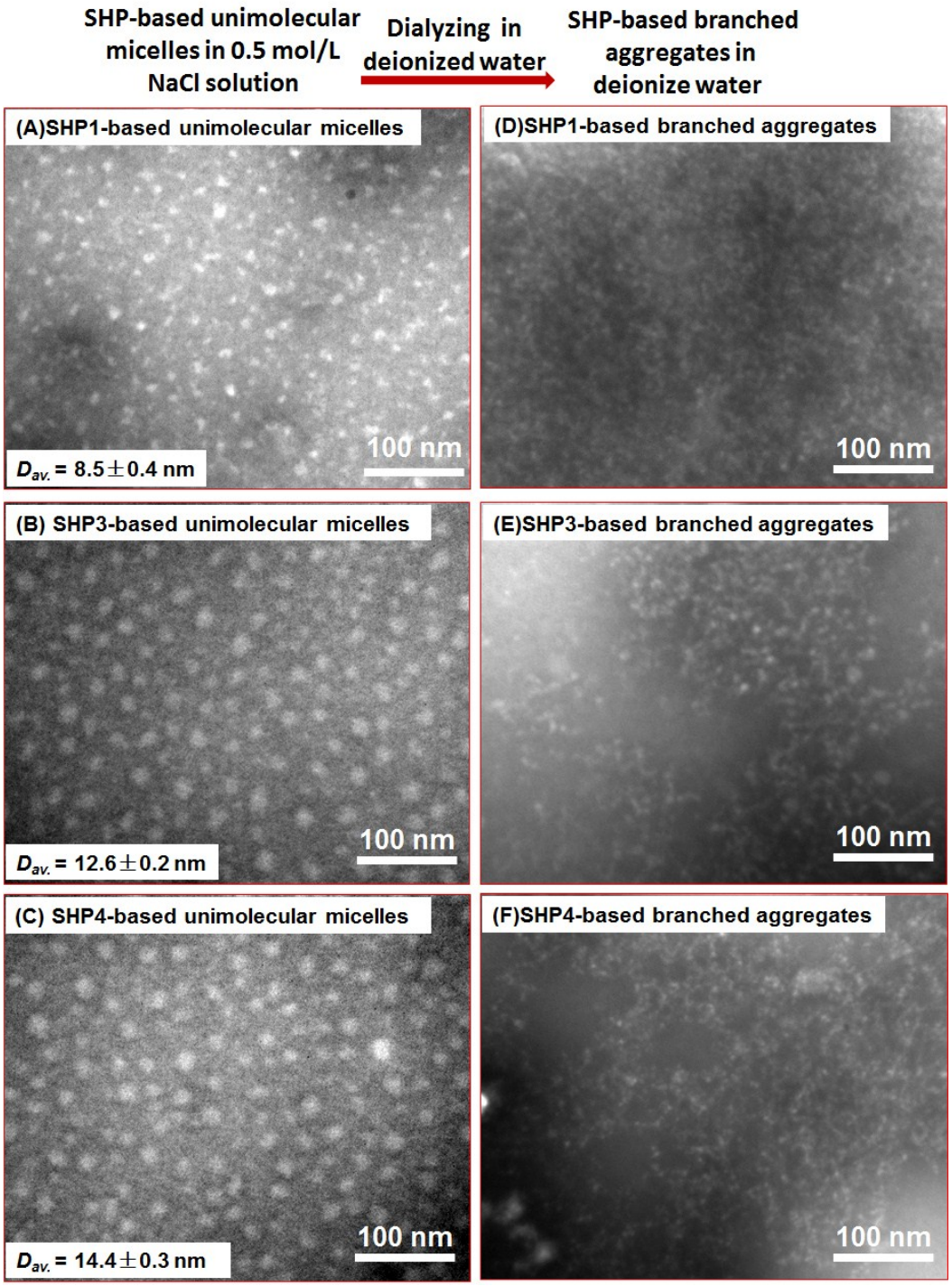

Figure S15 TEM images of SHP-based unimolecular micelles (A-C) formed in 0.5 mol/L NaCl solutions and SHP-based branched aggregates (D-F) formed in aqueous solutions.

Table S1 Structure parameters of SHP self-assemblies in differnt solution conditions at 25 °C.

Sample	Solution conditions[a]	$D_{av.,TEM}$[b] (nm)	D_h[c] (nm)	DPI[d]	M_w[e] (10^6 g/mol)	$A_{2,SPU}$[f] (10^{-5})	*dn/dc*[g]
SHP1-based unimolecular micelles	1	8.5±0.4	9.8±0.3	0.098±0.002	1.59±0.74	1.51±0.06	0.1326
SHP1-based unimolecular micelles	1	10.2±0.3	10.7±0.4	0.073±0.004	2.90±0.92	1.35±0.04	
SHP1-based unimolecular micelles	1	12.6±0.2	12.6±0.6	0.064±0.005	5.13±1.25	0.77±0.06	
SHP1-based unimolecular micelles	1	14.4±0.3	15.3±0.6	0.075±0.008	7.24±1.53	0.55±0.07	
SHP1-based branched aggregates	2	-	210±0.9	0.120±0.006	4.15±0.46	11.98±0.03	0.1827
SHP2-based branched aggregates	2	-	235±0.8	0.072±0.004	11.20±1.06	3.91±0.06	
SHP3-based branched aggregates	2	-	345±0.8	0.110±0.004	14.00±0.28	2.87±0.01	
SHP4-based branched aggregates	2	-	387±0.7	0.045±0.003	38.90±0.78	1.17±0.04	

[a] 1 and 2 repesent 0.5 mol/L NaCl solution and aqueous solution, respectively. [b] Average diameter determined by TEM. While $D_{av.,TEM}$ values of SHP self-assemblies in aqueous solutions can't be calculated by their TEM results due to the existence of branched morphology. [c] Hydrodynamic diameter determined by DLS. [d] Diameter distribution determined by DLS. [e] Apparent weight-average molecular weight (M_w) obtianed by Zimm plots determined by SLS. [f] Second virial coefficient (A_2) determined by SLS. [g] Average *dn/dc* values determined by refractive index detector.

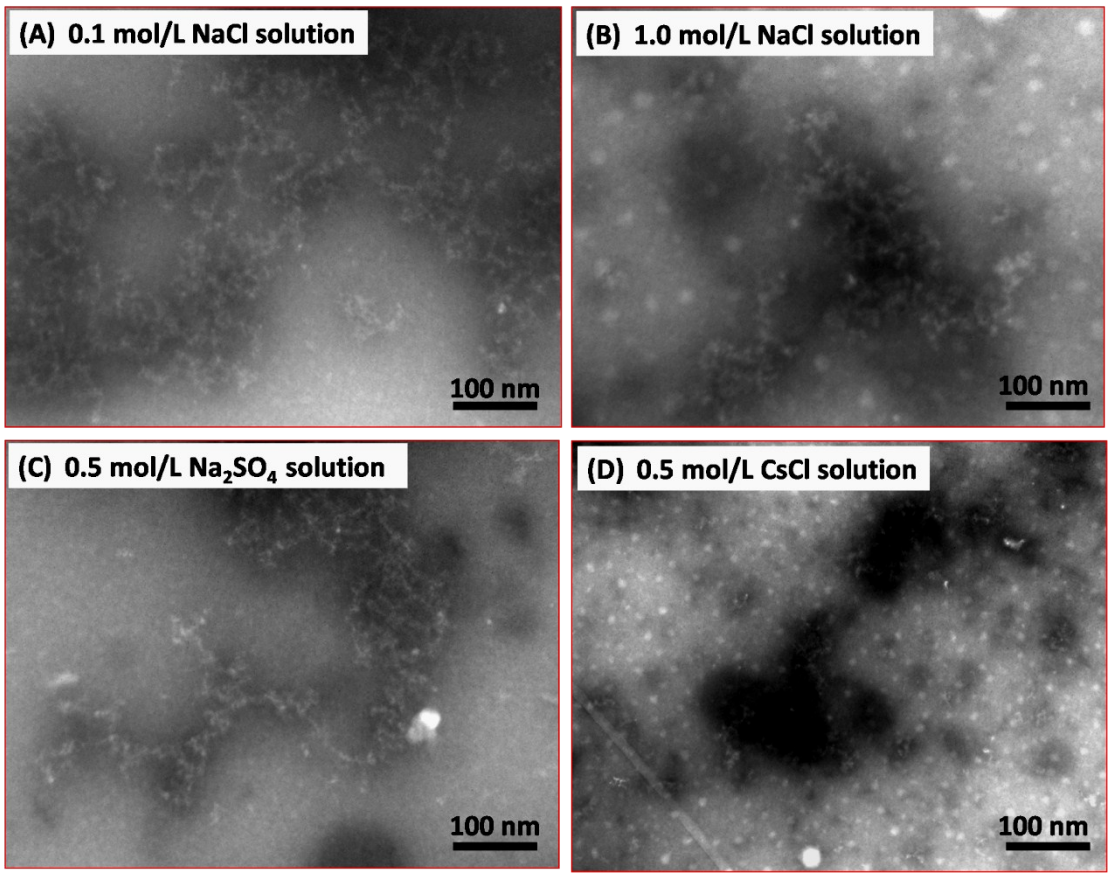

Figure S16 TEM images of SHP2-based self-assemblies in 0.1 mol/L NaCl solution (A), 1.0 mol/L NaCl solution (B), 0.5 mol/L Na_2SO_4 solution (C) and 0.5 mol/L CsCl solution (D). The concentration of the sample is set as 1.0 mg·mL^{-1}.

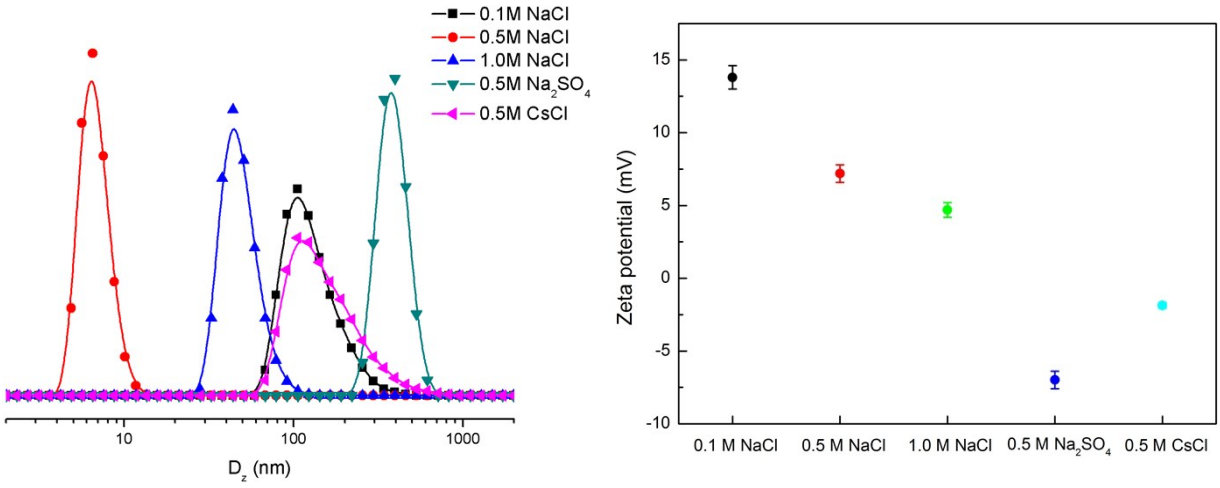

Figure S17 Size distributions and Zeta potentials of SHP2-based self-assemblies under different salt conditions.

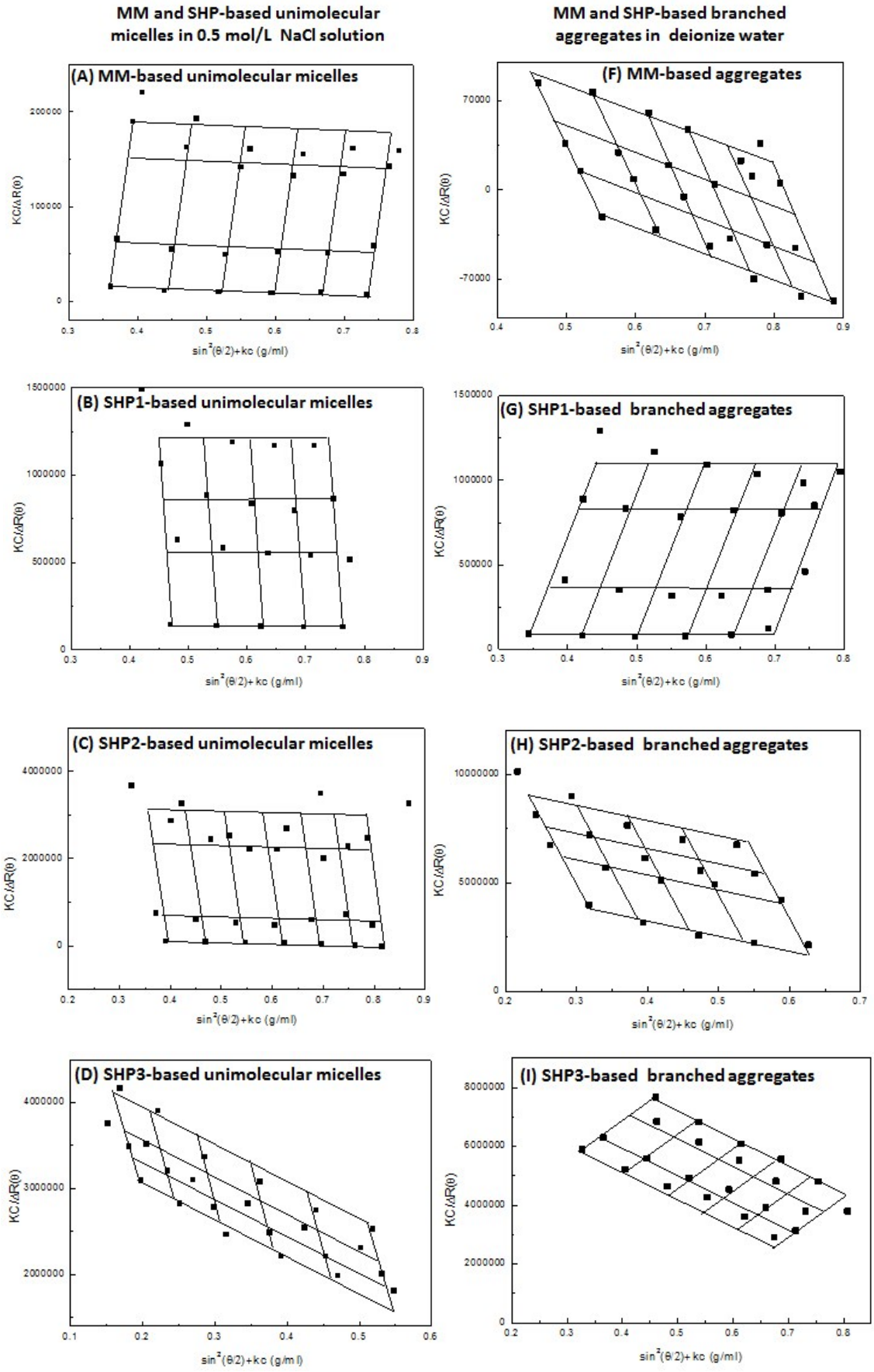
MM and SHP-based unimolecular micelles in 0.5 mol/L NaCl solution
MM and SHP-based branched aggregates in deionize water
(A) MM-based unimolecular micelles
(F) MM-based aggregates
(B) SHP1-based unimolecular micelles
(G) SHP1-based branched aggregates
(C) SHP2-based unimolecular micelles
(H) SHP2-based branched aggregates
(D) SHP3-based unimolecular micelles
(I) SHP3-based branched aggregates
KC/ΔR(θ)
sin²(θ/2)+kc (g/ml)

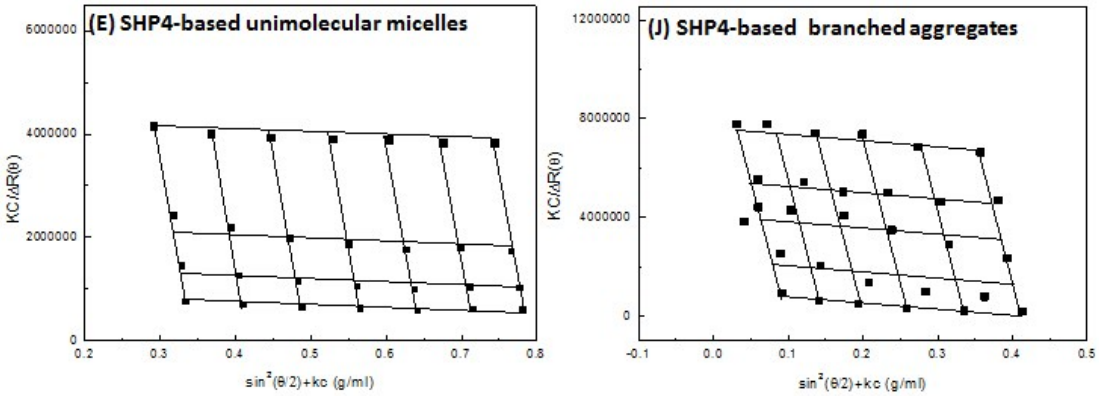

Figure S18 Zimm plots of MM and SHP self-assemblies in 0.5 mol/L NaCl solutions and aqueous solutions at 25 °C.

4. Reversibility of SHP self-assemblies

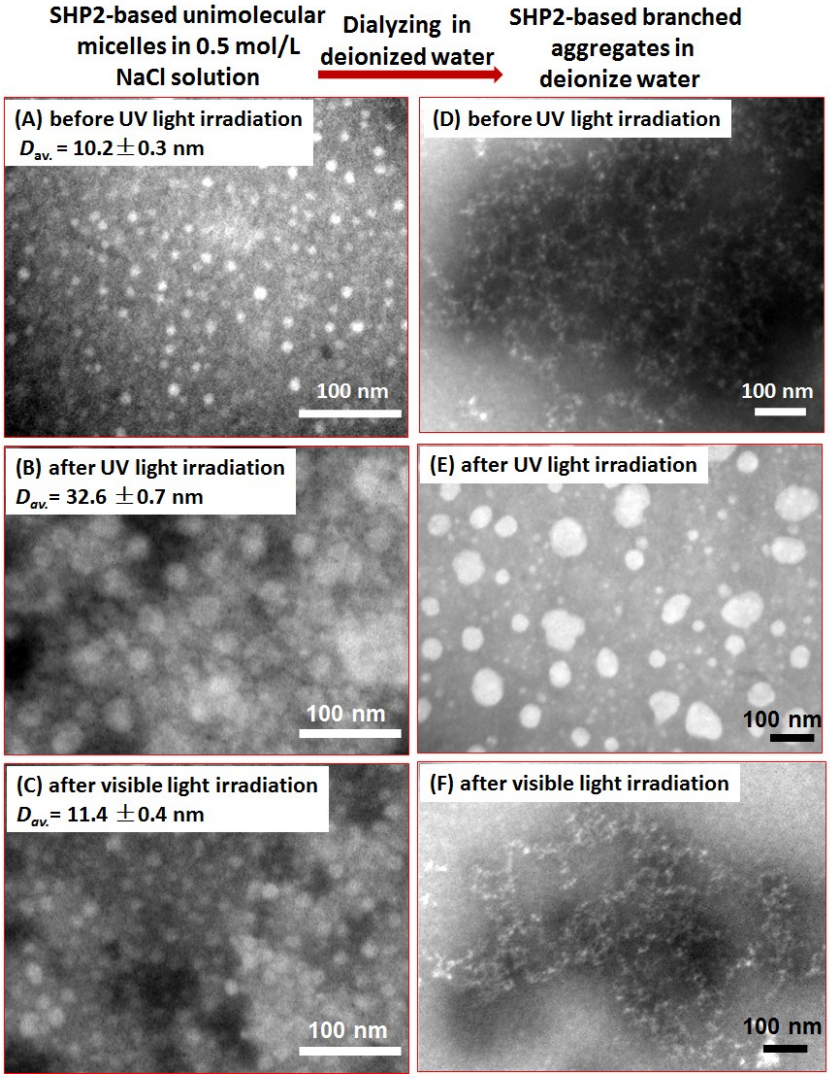

Figure S19 TEM images of SHP2-based unimolecular micelles in 0.5 mol/L NaCl solution (A-C) and SHP2-based branched aggregates in deionized water (D-F) at 25 °C, respectively. (A, D) Without irradiation; (B, E) After 365 nm UV irradiation for 20 min; (C, F) Subsequent visible light irradiation for 20 min.

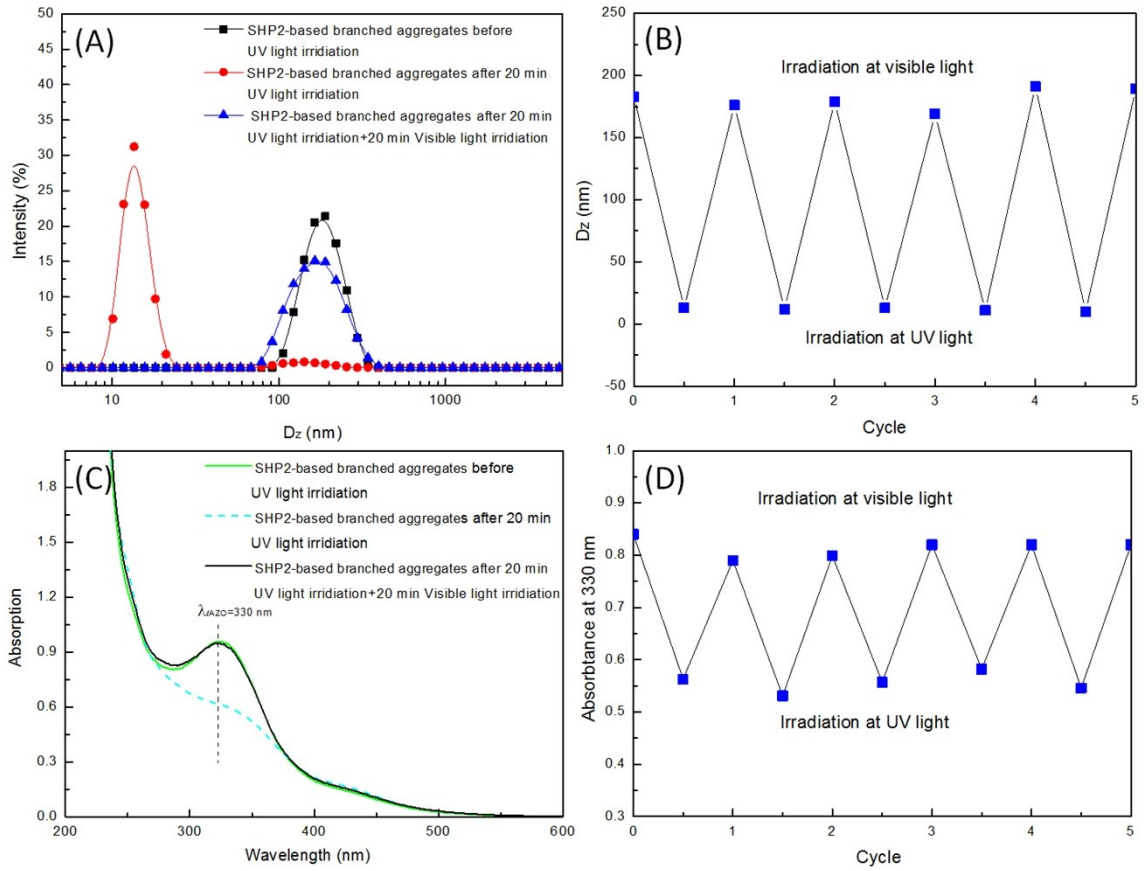

Figure S20 Confirmation of the reversibility of SHP2-based branched aggregates in deionized water. (A) D_z distribution of branched aggregates: before (black line) and after (red line) UV light irradiation, after UV and visible light irradiation (black line); (B) Cycle change of the D_z values of branched aggregates by alternately imposing UV and visible light irradiation; (C) UV-vis spectra of branched aggregates: before (green line) and after (blue line) UV light irradiation, after UV and visible light irradiation (black line); (D) Cycle change of the absorbance values at λ=330 nm of branched aggregates by alternately imposing UV and visible light irradiation.

5 Reference

[S1] J. T. Lai, D. Filla, R. Shea, *Macromolecules* **2002**, *35*, 6754.